Available online at www.sciencedirect.com
ScienceDirect
Minerals Engineering 20 (2007) 1121–1128
MINERALS ENGINEERING
This article is also available online at: www.elsevier.com/locate/mineng

An experimental investigation of foaming in acidic, high Fe_xO slags

S.A.C. Stadler, J.J. Eksteen *, C. Aldrich

Department of Process Engineering, University of Stellenbosch, Private Bag X1, Matieland, 7602 Stellenbosch, South Africa

Received 3 May 2005; accepted 28 January 2007
Available online 23 March 2007

Abstract

Slag foaming is common in pyrometallurgical processes, such as various non-ferrous operations like sulphide smelting/converting, base metal slag cleaning, steelmaking in basic oxygen furnaces, as well as in electric arc furnaces. Foaming phenomena remains poorly-understood. The purpose of this paper is to analyse the foaming behaviour of SiO_2–Al_2O_3–CaO–Fe_2O_3–FeO slags upon argon gas injection at various temperatures and slag chemistries, where the slag basicity and Fe_xO were varied. The results are interpreted in terms of physical properties, phase types and phase proportions that were predicted by models from literature. Foaming, as represented by a foam index, appeared to decrease with increasing basicity, until precipitation of solids had occurred. After this point, the foam index increased with increasing basicity. A few published empirical foaming models were statistically evaluated based on the measured foaming indices and physical property predictions, but no conclusive evidence could be found to justify the use of specific predictors of foaming such as bubble size or surface tension depression rather than surface tension.

Keywords: Slag foaming; Pyrometallurgy; Non-ferrous

1. Introduction

Slag foaming is common in melt systems where a significant amount of gas is produced, such as zinc fuming, carbothermic reduction reactions, hydrated and carbonate feed types which decompose when fed into molten slags, as well as converter systems where oxygen or air is injected into the melts (Morales et al., 1995; Mishra et al., 1998). If left unchecked, foaming can destabilise furnace operations. Unfortunately, the control of slag foaming is hampered by a lack of understanding of how fundamental factors, such as the physical properties of the slag, slag basicity or the presence of solids affect foaming. Ideally one would like to be able to control slag foaming within a typical operating region. Therefore, the influence of some of these factors on foaming in slags with high Fe_xO concentrations were considered, firstly with the aim of providing additional fundamental measurements and relationships, and secondly to evaluate some of the common empirical models as to their applicability to the slags systems studied.

Bikerman (1973) first considered the dynamic measurement of foamability, in which equilibrium between the formation and collapse of the foam is established by the constant rate generation of gas bubbles of a particular size. Eq. (1) defines the foam index as it is most commonly used in the study of slag foaming

$$\Sigma = \frac{\Delta H}{V} \tag{1}$$

where Σ is the foam index (s), ΔH is the change in liquid height (m), and V is the superficial gas velocity (m/s). Foam index values considered in this study ranged from 1.1 to 18.4 s. These values were within the range of foam index values previously reported for metallurgical slags of different compositions, ranging from 0.3 to 56 s (Roth et al., 1993; Zhang and Fruehan, 1995; Paramguru et al., 1997; Skupien and Gaskell, 2000). Despite many researchers using the foaming index as a measure of slag foaminess, it should be noted that the use of the foaming index

* Corresponding author. Tel.: +27 82 3766055; fax: +27 21 8082059.
E-mail address: jeksteen@sun.ac.za (J.J. Eksteen).

0892-6875/$ - see front matter © 2007 Elsevier Ltd. All rights reserved.
doi:10.1016/j.mineng.2007.01.013

remains controversial and that some authors rather prefer to use gas void fraction (Ogawa et al., 1993; Gou et al., 1996) or gas hold-up (Lin and Guthrie, 1995).

2. Experimental methods and materials

The experimental setup of the furnace with crucible and probe position is shown in Fig. 1. Experiments were performed in a neutral argon atmosphere in a Carbolite® STF 16/610 vertical tube furnace with silicon carbide heating elements. The recrystallized alumina tube has an inner diameter of 75 mm. The furnace provides a heated length of 610 mm and a uniform hot zone of 400 ± 5 mm. The long uniform hot zone temperature is important to provide uniform heating across the crucible length, while the long heated length aided in preheating the gas before injection in the slag melt. Ultra-high purity (UHP) argon gas was bubbled through the slag. The gas was introduced through a 820 mm long recrystallized alumina lance of 4.9 mm internal diameter. The room temperature gas flow was recorded based on calibrated rotameter readings.

Table 1 provides a summary of the experimental setups found in the literature for slag foaming measurements. These literature sources were used to plan the experimental setup used in this research.

The slags were contained in alumina crucibles, all of which had an inner diameter of 45 mm and a height of 280 mm. It was important to use very tall crucibles to allow for enough gas hold-up. Moreover, the crucible diameter had to be large to eliminate, as far as possible, wall effects of the crucible sides on the foam. Both the crucible height and diameter were comparable with the largest sizes reported in literature (Table 1). The crucible was wrapped in alumina wool around the top rim to keep it vertical for the duration of the experiment and stood on a pedestal made of alumina and supported by alumina tubes. The electrical probes were made of stainless steel. Foam heights were measured by lifting one probe gradually until electrical contact was broken (open circuit), which was taken as

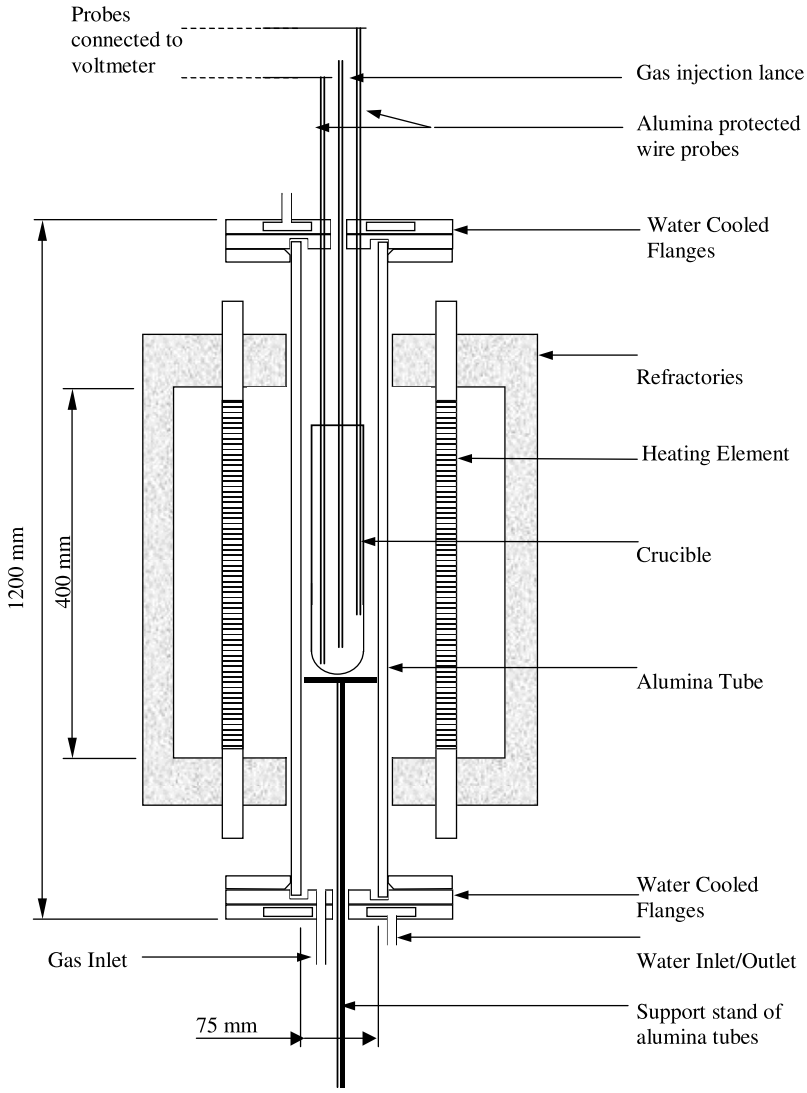

Fig. 1. Tube furnace setup for slag foaming determination.

Table 1
Summary of experimental setups to quantify slag foaming found in literature

Author	Crucible diameter (mm)	Crucible height (mm)	Crucible material	Probe material	Slag system	CaO/SiO_2 ratio	Atmosphere
Hara and Ogino (1990)	20	120	Alumina	Iron	$FeO–SiO_2–CaO$	–	Argon
Ito and Fruehan (1989)	32–50	200	Alumina	Stainless steel	$FeO–SiO_2–CaO$	0.43–1.00	Argon
Gudenau et al. (1992)	–	–	Alumina	–	$FeO–Fe_2O_3–SiO_2–CaO$	1.34–2.53	O_2 or N_2
Zamalloa et al. (1992a,b)	40	160	Alumina	Mo	$FeO–SiO_2–CaO$	0.4–1.0	Argon
Utigard and Zamalloa (1993)	40	160	Alumina	Mo	$FeO–SiO_2–CaO$	0.53–1.36	Argon
Koch and Ren (1994)	–	–	Graphite/ alumina	Photo-electric cell	$Fe_2O_3–SiO_2–CaO$	0.10–1.80	40% CO, 60% N_2
Ren et al. (1994)	–	–	Graphite	Photo-electric cell	$Fe_2O_3–SiO_2–CaO$	0.10–2.70	40% CO, 60% N_2
Zhang and Fruehan (1995)	41–50	–	Alumina	Mo	$CaO–SiO_2–CaF_r$	0.50	Argon
Ozturk and Fruehan (1995)	41	300	Alumina	Mo	$CaO–SiO_2–Al_2O_3–FeO$	–	Argon
Yi and Rhee (1997)	40	200	MgO or graphite	X-ray fluoroscopy	$FeO–SiO_2$	–	–

the maximum height of the foam. The slags were prepared from analytically pure SiO_2, CaO, Al_2O_3 and Fe_2O_3. The Fe_xO was prepared from premixed ratio's of Fe and Fe_2O_3 which were pre-reacted as compacted pellets in a vertical tube furnace at 900 °C for 10 h in an argon atmosphere. The Fe_xO was stored in a dry, non-oxidising atmosphere, until it was used in the experimental work. The master slags (excluding Fe_xO) were pre-melted in an induction furnace using a graphite crucible as susceptor. The master slags were then pulverised, remelted, and pulverised again, after which it was left for 9 h in a muffle furnace to burn off any traces of residual carbon. The pulverised slags were subsequently mixed with the separately prepared Fe_xO and remelted in the tube furnace under a UHP argon atmosphere, after which additional UHP argon was introduced via the lance, allowing an 8 h melting time before gas injection. Gas injection was maintained until a steady reading was obtained for foam height. The compositions of the slags, temperatures, as well as the foam indices measured with each slag are summarized in Table 2. All the Fe_2O_3, and FeO are lumped together as total Fe in the form of Fe_xO in Table 2. The Fe^{3+}/Fe^{2+} ratios (as determined by titration) of the slags are also presented in Table 2. The compositions of the slags were determined by XRF analyses, and the Fe^{2+}/Fe^{3+} ratios of the slags were determined by the hot acid titration method (where $K_2Cr_2O_7$ was used to indicate the critical point of the titration).

One of the limitations of the experimental setup was found to be excessive foaming of the slag, which led to slag overflow. This in turn made the removal of the crucible difficult, as it tended to cement the crucible to the furnace tube. Moreover, prolonged contact with the slag weakened the furnace tube and eventually leads to irreparable damage. Therefore, if any foaming were detected within 5 cm from the top of the crucible, the experiment would be interrupted and continued at a lower gas velocity or different temperature in an effort to avert slag overflow. While X-ray diffraction analyses of the slags would have been very useful to confirm the presence of mineralised species, the results would have been misleading due to the slow cooling that the crucible undergoes before removal from the

Table 2
Average foam index values for metallurgical slags

Slag no.	Temperature (K)	Composition (wt%)					Foam index (s)
		SiO_2	Al_2O_3	CaO	Total Fe as Fe_xO	Fe^{2+}/Fe^{3+}	
1	1448	45.5	10.5	20.3	23.7	7.1	1.6
1	1473	45.5	10.5	20.3	23.7	7.1	1.2
1	1498	45.5	10.5	20.3	23.7	7.1	1.1
2	1413	47.5	9.7	20.0	22.8	10.6	3.6
2	1438	47.5	9.7	20.0	22.8	10.6	2.0
2	1463	47.5	9.7	20.0	22.8	10.6	3.4
3	1413	41.4	6.0	32.8	19.9	4.7	9.6
3	1438	41.4	6.0	32.8	19.9	4.7	8.1
3	1463	41.4	6.0	32.8	19.9	4.7	16.3
4	1384	45.1	7.1	19.8	28.0	5.3	5.4
4	1409	45.1	7.1	19.8	28.0	5.3	4.6
4	1434	45.1	7.1	19.8	28.0	5.3	3.9
5	1473	41.0	15.4	17.8	25.9	0.7	1.9
5	1498	41.0	15.4	17.8	25.9	0.7	2.1
5	1523	41.0	15.4	17.8	25.9	0.7	2.6
5	1573	41.0	15.4	17.8	25.9	0.7	16.3
5	1623	41.0	15.4	17.8	25.9	0.7	18.4
6	1448	53.5	6.8	19.3	20.4	12.9	6.9
6	1498	53.5	6.8	19.3	20.4	12.9	6.6
7	1573	46.9	19.2	9.7	24.2	21.2	7.9
7	1613	46.9	19.2	9.7	24.2	21.2	4.1
7	1638	46.9	19.2	9.7	24.2	21.2	4.1
7	1653	46.9	19.2	9.7	24.2	21.2	9.0
8	1623	43.8	5.0	25.3	25.0	24.0	6.2
8	1673	43.8	5.0	25.3	25.0	24.0	10.4
9	1573	51.9	10.0	28.8	9.3	35.5	9.0
10	1673	52.9	8.4	24.8	13.9	32.7	8.2
11	1673	42.8	17.1	31.5	8.6	30.7	4.5

Table 3
Physical properties of the metallurgical slags investigated

Slag index	Temperature (K)	Density (kg/m^3)	Viscosity (Pa s)	Surface tension (N/m)
1	1448	3089	5.53	0.469
1	1473	3095	4.18	0.460
1	1498	3102	3.14	0.451
2	1413	3072	8.58	0.475
2	1438	3076	6.50	0.468
2	1463	3081	4.94	0.461
3	1413	3142	12.96	0.513
3	1438	3121	8.19	0.501
3	1463	3106	4.33	0.486
4	1384	3097	7.91	0.482
4	1409	3101	6.04	0.475
4	1434	3106	4.36	0.468
5	1473	3168	7.09	0.483
5	1498	3160	5.43	0.577
5	1523	3151	4.35	0.470
5	1573	3185	1.61	0.493
5	1623	3185	1.61	0.486
6	1448	3005	5.58	0.446
6	1498	3005	5.58	0.438
7	1573	3135	5.46	0.467
7	1613	3135	5.46	0.461
7	1638	3135	5.46	0.457
7	1653	3135	5.46	0.455
8	1623	3121	0.90	0.480
8	1673	3121	0.90	0.473
9	1573	2899	7.26	0.457
10	1673	2941	6.18	0.438
11	1673	2952	4.12	0.473

furnace. Quenching (to preserve the high temperature equilibrium phases) was not done due to the size of the crucible, which contained about 500 g of slag. Attempted quenching of this amount of hot slag would have lead to unsafe working conditions. The size of the crucible would further have lead to additional non-equilibrium effects as rapid quenching becomes impossible due to the formation of an insulating freeze layer at the slag-gas and slag-crucibles interfaces.

2.1. Prediction of physical properties

The predicted physical properties of the slags are summarized in Table 3. The density predictions are obtained based on partial molar volume predictions and the surface tension is similarly based on partial molar surface tensions of the components. In both cases, the estimation formulas used by Zhang (1992) for his slag foaming research were also used in this work. The viscosities of completely liquid slags were determined from a modified Urbain equation, as presented by Kondratiev and Jak (2001). The calculations of the physical properties are given by Stadler (2002).

3. Results and discussion

3.1. Effect of basicity on slag foaming

The foam index decreased with increasing basicity, owing to the lowering of the slag viscosity arising from the break-up of the silicate polymers in the slag. This trend continued until a point where solids were predicted to start precipitating from the slag, at which point the trend reversed and the foam index increased with further increases in the basicity of the slag. These observations were in line with those of Ito and Fruehan (1989), who observed that minimal foaming took place with a $CaO/(SiO_2 + Al_2O_3)$ weight-to-weight ratio of approximately 1.2. Their slags contained 30 wt% FeO and 3–5 wt% Al_2O_3 and were studied over a temperature range of 1576 K and 1673 K.

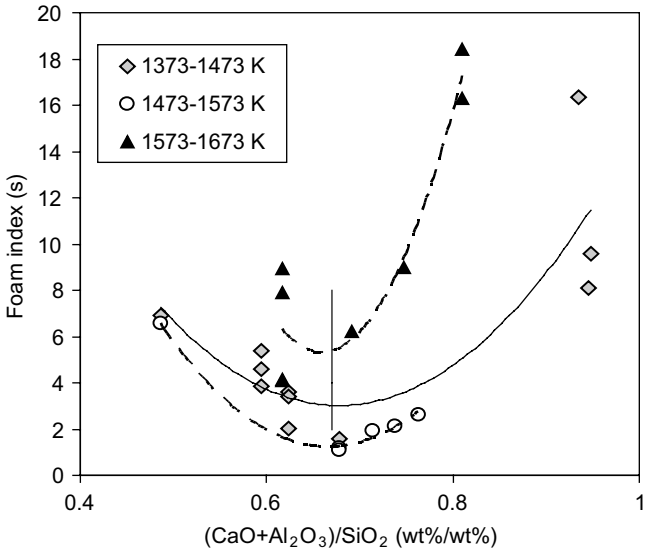

Fig. 2. Effect of temperature and basicity on the foam index.

Fig. 2 shows the point of minimum foaming at a $(CaO + Al_2O_3)/SiO_2$ weight-to-weight ratio of approximately 0.67. The difference between this ratio and the one found by Ito and Fruehan (1989) can be explained by the difference in Al_2O_3 concentration in the slag and the presence of Al_2O_3 in the denominator, rather than the numerator of the basicity expression. A higher level of Al_2O_3 decrease the composition range of the fully liquid zone at the operating temperatures and therefore leads to solids precipitation at lower slag basicity. Alumina was used in the numerator of the basicity expression (rather than its usual position in the denominator), as its amphoteric nature makes it behave like a base in the acidic slags studied in this work. On the other hand, Ito and Fruehan (1989) performed their experimental investigations with basic slag chemistries as found in steelmaking.

3.2. Effect of Fe_xO concentration on foaming in slags

Work done by Jiang and Fruehan (1991) has indicated that the foam index decreases with an increasing FeO content (ranging from 2 to 15 wt% FeO) and CaO/SiO_2 weight-to-weight ratios of 1.0–1.25. This can probably be attributed to the lower liquid viscosity associated with an increased FeO concentration. Fig. 3 shows that the influence

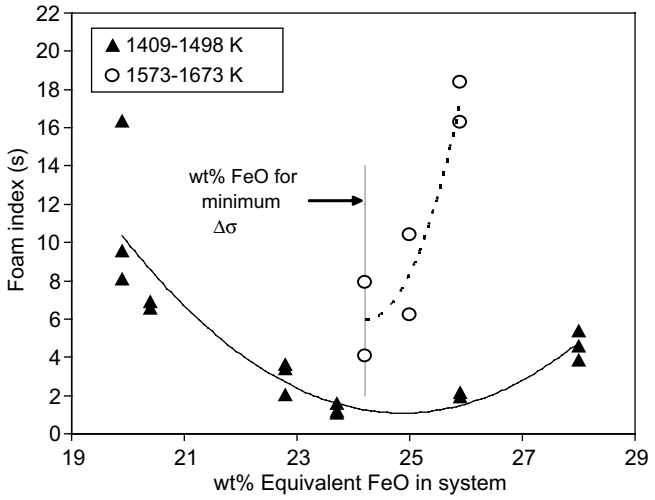

Fig. 3. Foaming characteristics for varying Fe_xO concentrations at temperature ranges 1409–1498 K (triangles) and 1573–1673 K (circles).

of FeO concentration reaches a minimum at approximately 25 wt% FeO. The operating temperatures were significantly above the slag liquidus temperatures in all the cases presented in Fig. 3.

3.3. Surface tension and surface tension depression

Use of the surface tension depression, rather than the surface tension itself as a predictor of slag foaming has been proposed by Ghag et al. (1998a,b). The surface tension depression is the slope of the curve obtained when the surface tension is plotted against the molar concentration of the surface active element, that is $|\partial\sigma|/\partial$(mole Fe_xO). In a multi-component system it is difficult to determine the effect of surface tension depression at a given composition and/or temperature, mainly because it is difficult to vary other influential factors independently.

A minimum value of 464 ± 4 mN/m in surface tension was noted at an Fe_xO mole fraction of 0.228 for the slags under investigation as depicted in Fig. 4. The minimum noted in surface tension depression also corresponds with a minimum point in the foam index versus Fe_xO concentration, shown in Fig. 3. It can therefore be concluded that while an increase of Fe_xO concentration lowers the viscosity of slags and this leads to a decrease in the foam index, the surface tension depression varies with Fe_xO concentration and this can lead to an increase in the foam index, overriding the lowering in slag viscosity (and hence less foaming) associated with increased Fe_xO concentrations.

Calculations indicated that the surface tension depression for Fe_xO was constant at a given basicity and fixed Al_2O_3 and Fe_2O_3 levels. For illustrative purposes, Fig. 5 shows the calculated change in surface tension by Fe_xO annotated in a greyscale envelope for acid and basic slags. An impurity level of 3% Fe_2O_3 was used as the basis for these calculations. It is clear that the surface tension depression is more pronounced for acidic slags and would therefore have greater influence over the foaming behaviour of acidic slags than basic slags.

3.4. Effect of solid precipitates on slag foaming

The XRF-determined slag composition data (of the resulting slags after gas injection) were used in thermodynamic simulations (FactSage®) to predict the amount of solids present in the melt at the different temperatures of interest. Although no XRD analysis were done to confirm the presence and quantity of the predicted phases, due to the reservations presented in Section 2, the long heating times, and preprocessing for homogenisation (multiple remelting and pulverisation) was assumed to be sufficient to establish equilibrium conditions. The predicted phases of solid particles agreed with the $FeO–Fe_2O_3–SiO_2–CaO–Al_2O_3$ multi-component phase diagrams by Kongoli and

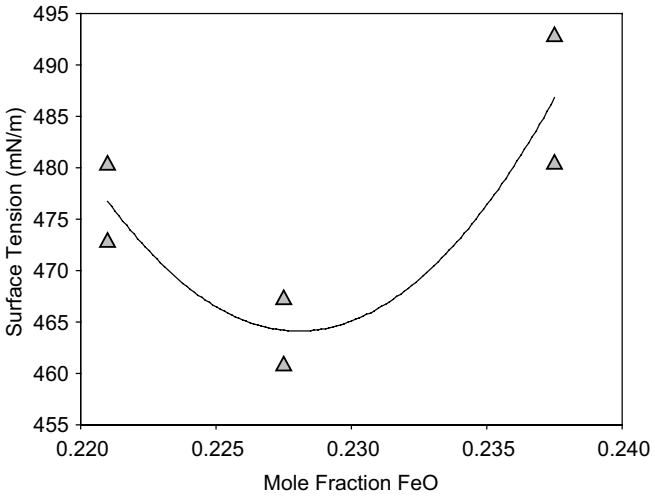

Fig. 4. Surface tension values (solid triangles) with trend line (solid line) for slags at temperatures of 1573 K and 1673 K.

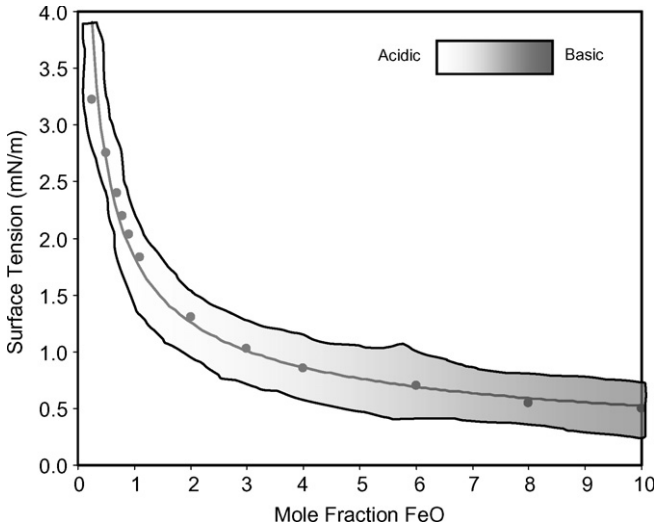

Fig. 5. Estimated surface tension for various basicity levels at 1500 °C and 5% Al_2O_3.

Yazawa (2001). The predicted apparent viscosity of the slag (Eq. (2)) took into account the effect of solids according to the model suggested by Happel (1957)

$$\frac{\mu}{\mu_0} = 1 + 5.5 \cdot \varphi \cdot \psi \tag{2}$$

where φ is the volume fraction of solids in the melt, ψ is an interaction factor dependent on the solids concentration, μ is the adjusted viscosity of the melt, and μ_0 is the viscosity of the melt without any solids. These viscosities were determined from a modified Urbain model published by Kondratiev and Jak (2001).

The densities of the solid precipitates were obtained from the FactSage® database, except for the density of magnetite (Fe_3O_4) where the values published by Gray (1971) were used. For the slag systems and temperatures used in this work, the precipitates were predicted to be one or more of magnetite, wollastonite (Fe_3O_4, $CaSiO_3$) or anorthite ($Ca_2Al_2SiO_7$). Finally, the volume fractions of the solids in the melt were calculated from the densities of the precipitates, as well as the masses of the solid precipitates estimated by FactSage®.

Fig. 6 suggests an increase in the slag foam index with an increase in the predicted total amount of solids. Small volume percentage magnetite in the slag stabilised the foaming, but increasing amounts of wollastonite and anorthite appeared to destabilise foaming. The influence of solids on foaming is therefore complicated not only by the amount of solids present in the system, but also of the nature of the solids. Magnetite (s.g. of 5.2) has a isometric cubo-octahedral crystal structure, while both wollastonite (s.g. between 2.87 and 3.09) and anorthite (s.g. between 2.74 and 2.76) crystallize in needle-like triclinic crystals. Their needle-like nature may have caused foam destabilisation, but this needs to be validated in further studies. In theory, the more bulky (lower density) needle-like crystals of anorthite and wollastonite may form crystal bridges between the bubble surfaces, thereby increasing the lamellar cross-sectional areas for liquid drainage, while the much denser (and smaller) magnetite does not have the same effect. In contrast, through increasing the observed viscosity of the melt, the magnetite may retard drainage and stabilise the slag foam. However, more experimental work is again required, investigating crystal type, wettability, size and density before this hypothesis can be validated.

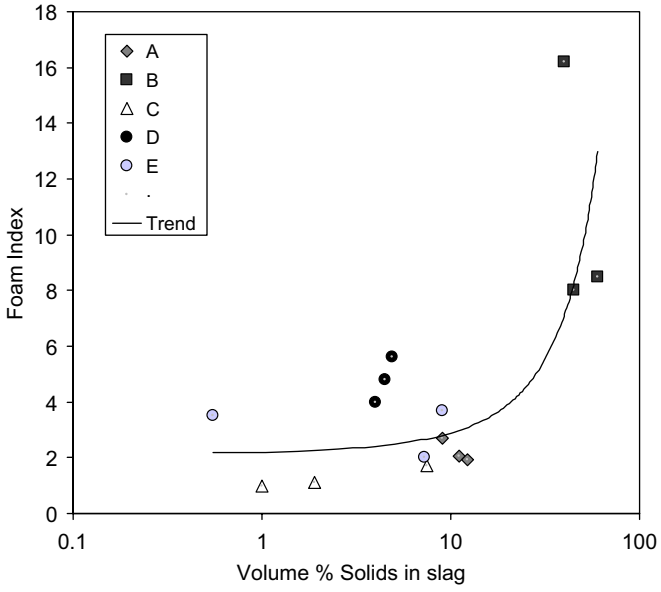

Fig. 6. Influence of solid precipitates on slag foaming: (A) anorthite and magnetite, 1448–1523 K, (B) wollastonite and magnetite (1413–1463 K), (C) magnetite (1448–1489 K), (D) magnetite (1384–1434 K) and (E) magnetite (1413–1463 K).

4. Slag foam models

Three models were selected to see to what degree they could explain the influence of the physical properties of the slags on the average foam index. These models generally considered the relationships between the slag variables, such as slag density, viscosity an surface tension or surface tension depression and the foam index, and in some cases also the size of gas bubbles in the slags, as outlined in more detail below.

4.1. Model of Jiang and Fruehan (1991)

Jiang and Fruehan considered the relationship between two dimensionless numbers, viz. $N_1 = \Sigma g\mu/\sigma$ and $N_2 = \rho\sigma^3/\mu^4 g$. In order to test the empirical models, the data were fitted in the form of power law relationships:

$$\Sigma g\mu/\sigma = K(\rho\sigma^3/\mu^4 g)^n \tag{3}$$

Models (Eqs. (4) and (5)) were fitted separately for basic and acidic slags and yielded the following results after simplification:

$$\text{Basic slags: } \Sigma = 115\frac{\mu}{\sqrt{\rho\sigma}} \tag{4}$$

$$\text{Acidic slags: } \Sigma = 0.93\frac{\mu}{\rho^{2/3}\sigma} \tag{5}$$

The model (Eqs. (4) and (5)) did not explain the foaming behaviour of acidic slags well. Reasons for this might be uncertainties associated with in the measured or predicted slag properties, but possibly also the fact that the model relied on the surface tension of the slag, rather than surface tension depression.

4.2. Model of Zhang and Fruehan (1995)

Zhang and Fruehan (1995) have proposed models similar to those of Jiang and Fruehan, but recommended inclusion of bubble size as well. The model was fitted to data for slags with a unity ratio of CaO/SiO_2 that contained 5–15 wt% Fe_xO at 1500 °C. This gave a model of the form shown in Eq. (6) for basic slags and Eq. (7) for acidic slags:

$$\text{Basic slags:} \quad \Sigma = 115\frac{\mu^{1.2}}{\sigma^{0.2}\rho D_b^{0.9}} \tag{6}$$

$$\text{Acidic slags:} \quad \Sigma = 10.3\times 10^4\frac{\sigma^{12}}{\mu^{0.4}\rho^{11.7}D_b^{23}} \tag{7}$$

The importance of the different variables in Eqs. (6) and (7) as related to the foam index differs markedly. Eq. (6) indicates that the slag viscosity is the variable with the most influence on the foam index values and the slag surface tension the variable with the least influence. In contrast, Eq. (7) gives the bubble size and the slag surface tension as the variables with the largest influence on the foam index, while the slag viscosity is deemed less important.

4.3. Model of Ghag et al. (1998a,b)

Ghag et al. (1998a,b) have models similar to those of Jiang and Fruehan (1991) and Zhang and Fruehan (1995), except that they had considered the surface tension depression, instead of the surface tension itself. In order to fit the model, it was assumed that the surface tension depression could be described by the difference between the surface tension of the slag and the surface tension of pure SiO_2 at similar conditions. SiO_2 were chosen as the pure liquid, as it was the component with the highest concentration in the slag. This yielded the relationship presented by Eq. (8), with $k = 7\times 10^{13}$ and $\delta = 7.57$ for acidic slags:

$$\frac{\Sigma\Delta\sigma}{\mu D_b} = k\left(\frac{\Delta\sigma}{\rho g D_b^2}\right)^{\delta} \tag{8}$$

Scatter plots of the model predictions versus measured foam indices are shown in Fig. 7, where the Ghag's model (1998a,b) is compared with the one proposed by Zhang and Fruehan (1995). A diagonal line is included to show the deviation from the perfect model. Although the fits of the models differ in terms of their Pearson correlation coefficients (r), it can be shown that these differences are not statistically meaningful. That is, testing the null hypothesis that the results obtained with the three models described above do not differ significantly, can be done by first transforming the Pearson's correlation coefficients by use of the well-known Fisher's z-transformation (Kreyszig, 1970) so that they are approximately normally distributed and then approximating the sampling distribution of the difference between two correlation coefficients in terms of these z-values (see Eq. (9) below). The hypothesis that these differences are not statistically different from zero is then tested. The calculations are summarized by Eqs. (9)–(11):

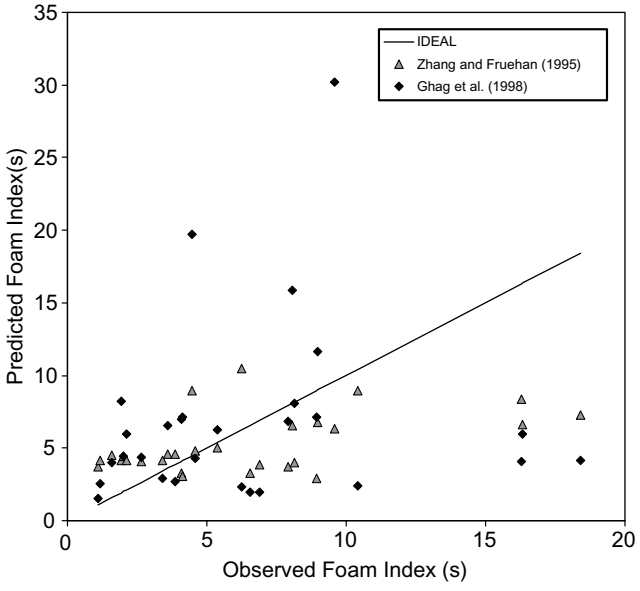

Fig. 7. Comparison of the models proposed by Zhang and Fruehan (1995) and Ghag et al. (1998a,b).

$$z = (Z_1 - Z_2 - \omega_{\Delta z})/\sigma_{\Delta z} \tag{9}$$

where

$$Z_j = \frac{1}{2}\ln\{(1 + r_j/1 - r_j)\} \tag{10}$$

and

$$\sigma_{\Delta z} = (2/N)^{1/2}, \tag{11}$$

the standard deviation of the differences between Z_1 and Z_2

and $\omega_{\Delta z}$ is the difference between means Z_1 and Z_2, using the same data set with $N = 28$ samples for all the models.

Denoting the correlation coefficients of the three models as $r_J = 0.53$ (Jiang and Fruehan, 1991), $r_Z = 0.66$ (Zhang and Fruehan, 1995) and $r_G = 0.72$ (Ghag et al., 1998a,b), then $Z_J = 0.591$, $Z_Z = 0.785$, $Z_G = 0.910$, $\omega_{\Delta z} = 0$ and $\sigma_{\Delta z} = 0.302$ for all the models.

Considering the null hypothesis that H_0: $\omega_{\Delta z} = 0$ (the models do not differ significantly), as opposed to the alternative hypothesis that H_A: $\omega_{\Delta z} \neq 0$ (the models differ significantly), it can be seen that $z_{JZ} = 0.642$, $z_{JG} = 1.06$, $z_{ZG} = 0.413$. The absolute values of these differences are all smaller than the critical value of 1.96 (two-tailed test at a 95% significance level), so the null hypothesis that the models are not statistically different cannot be rejected.

5. Conclusions

While some general trends could be observed for three-phase slag systems, foaming could not be described completely in terms of the slag rheology and measured operating conditions. The fact that the foaming behaviour of three-phase melt-solids–gas systems are still not well understood, underscores the need for experimental data, to which this paper makes a contribution. As the froth stability is strongly dependent on the physical properties, and as they all vary simultaneously with a change in chemistry of temperature, it further complicates research in this field as the properties cannot be varied one at a time. However,

from this study, a number of qualitative observations can be made:

- Increasing Fe_xO concentrations decreased the foam index, apparently by lowering the viscosity of the slag. However, at high Fe_xO concentrations, higher surface tension depression associated with increased concentrations of Fe_xO may have led to increased foaming. The foam stability was therefore not a monotonic function of Fe_xO concentration, but showed a point of minimum stability.
- The foam index decreased with increasing basicity until a point is reached which coincides with anticipated solids precipitation. After this point, the foam index increased with increasing basicity. It is therefore thought that while the slag is completely fluid, the effect of basic oxides is to depolymerise the slag, leading to a decreased viscosity, faster drainage from the foam lamellae and consequently lower foam stabilities, until such a point where the predicted solids precipitation increases the apparent viscosity of the melt and slows down interlammellar drainage, thereby increasing froth stability.
- Three different models proposed by previous authors were fitted to the data, but no conclusive statistical evidence to justify the use of bubble size or surface tension depression, instead of surface tension, as predictors of foaming could be found.
- An predicted increase in the solid precipitates in the slag appeared to increase foam stability. This observation has to be qualified in that other properties of the slag may result in the precipitates have a different net effect on the formation of foam. For example, the precipitation of isometric, surface-active magnetite led to foam stabilisation, while increasing amounts of non-isometric particles appeared to have no effect or even a slightly destabilising one.

Acknowledgements

The authors would like to express their gratitude towards Mintek who sponsored the research work of Ms. Stadler towards obtaining her M.Sc. (Eng) at the University of Stellenbosch. This paper is published from the results obtained by Stadler (2002) in her M.Sc.

References

Bikerman, J.J., 1973. Foams. Springer-Verlag, New York, NY, USA.

Ghag, S.S., Hayes, P.C., Lee, H., 1998a. Physical model studies on slag foaming. ISIJ International 38 (11), 1201–1207.

Ghag, S.S., Hayes, P.C., Lee, H., 1998b. Model development of slag foaming. ISIJ International 38 (11), 1208–1215.

Gou, H., Irons, G.A., Lu, W.-K., 1996. A multiphase fluid mechanics approach to gas hold-up in bath smelting processes. Metallurgical and Materials Transactions B 27 (2), 195–201.

Gray, T.J., 1971. Oxide spinels. In: Alper, A.M. (Ed.), In: High Temperature Oxides, 5-IV. Academic Press, New York, London, p. 97.

Gudenau, H.W., Wu, K., Nys, S., Rosenbaum, H., 1992. Formation and effect of slag foaming in smelting reduction. Steel Research 63 (12), 521–525.

Happel, J., 1957. Viscosity of suspensions of uniform spheres. Journal of Applied Physics 28 (11), 1288–1292.

Hara, S., Ogino, K., 1990. The surface viscosities and the foaminess of molten oxides. ISIJ International 30 (9), 714–721.

Ito, K., Fruehan, R.J., 1989. Study on the foaming of $CaO–SiO_2–FeO$ slags. Metallurgical and Materials Transactions B 20B, 509–514.

Jiang, R., Fruehan, R.J., 1991. Slag foaming in bath smelting. Metallurgical and Materials Transactions B 22B, 481–489.

Koch, K., Ren, J., 1994. Photoelectric measurement of the foaming process in the reduction of slags containing iron oxide. Steel Research 65 (1), 3–7.

Kondratiev, A., Jak, E., 2001. Review of experimental data and modelling of the viscosities of fully liquid slags in the $Al_2O_3–CaO–FeO–SiO_2$ system. Metallurgical and Materials Transactions B 32B, 1015–1025.

Kongoli, F., Yazawa, A., 2001. Liquidus surface of $FeO–Fe_2O_3–SiO_2–CaO$ slag containing Al_2O_3, MgO, and Cu_2O at intermediate oxygen partial pressures. Metallurgical and Materials Transactions B 22B, 583–592.

Kreyszig, E., 1970. Introductory Mathematical Statistics: Principles and Methods. John Wiley & Sons, New York, NY, pp. 343–347.

Lin, Z., Guthrie, R.I.L., 1995. A model for slag foaming for the bath smelting process. Iron and Steelmaker 22 (5), 67–73.

Mishra, P., Deo, B., Chabra, R.P., 1998. Dynamic model of slag foaming in oxygen steelmaking converters. ISIJ International 38 (11), 1225–1232.

Morales, R.D., Ruben Lule, G., Lopez, F., Camacho, J., Romero, J.A., 1995. The slag foaming practice in EAF and its influence on the steelmaking shop productivity. ISIJ International 35 (9), 1054–1062.

Ogawa, Y., Gaye, D.H.H., Tokumitsu, N., 1993. Physical model of slag foaming. ISIJ International 33 (1), 224–232.

Ozturk, B., Fruehan, R.J., 1995. Effect of temperature on slag foaming. Metallurgical and Materials Transactions B 26B (5), 1086–1087.

Paramguru, R.K., Galgali, R.K., Ray, H.S., 1997. Influence of slag and foam characteristics on reduction of FeO-containing slags by solid carbon. Metallurgical and Materials Transactions B 28B, 805–810.

Ren, J., Westholt, M., Koch, K., 1994. Influence of MgO, K_2O, Na_2O and gas pressure on slag foaming behaviour under reducing conditions. Steel Research 65 (6), 213–218.

Roth, R.E., Jiang, R., Fruehan, R.J., 1993. Foaming of ladle and BOS-Mn smelting slags. ISS Transactions 14, 95–103.

Skupien, D., Gaskell, D.R., 2000. The surface tensions and foaming behaviour of melts in the system $CaO–FeO–SiO_2$. Metallurgical and Materials Transactions B 31B, 921–925.

Stadler, S.A.C., 2002. An experimental study of slag foaming. MSc Dissertation. Department of Process Engineering, University of Stellenbosch.

Utigard, T.A., Zamalloa, M., 1993. Foam behaviour in liquid ferrous oxide–calcia–silica slags. Scandinavian Journal of Metallurgy 22 (2), 83–90.

Yi, S.-H., Rhee, C.-H., 1997. Effects of additives on the foaming behaviour of $FeO–SiO_2$ based slags. Steel Research 10, 429–433.

Zamalloa, M., Warczok, A., Utigard, T.A., 1992a. Slag foam formation and stability. In: EPD Congress 1992, Proceedings of the TMS Annual Meeting 1992, pp. 931–943.

Zamalloa, M., Warczok, A., Utigard, T., 1992b. Slag foaming during gas injection. In: Electric Furnace Conference Proceedings, vol. 49, pp. 197–204.

Zhang, Y., 1992. Slag Foaming in the Bath-Smelting Process. Department of Materials Science and Engineering, Carnegie Mellon University, Pittsburg, PY, p. 164.

Zhang, Y., Fruehan, R.J., 1995. Effect of bubble size and chemical reactions on slag foaming. Metallurgical and Materials Transactions B 26B, 803–812.